Improvement of Predictive Current Control Performance Using Online Parameter Estimation in Phase Controlled Rectifier

Se-Jong Jeong, *Student Member, IEEE*, and Seung-Ho Song, *Member, IEEE*

***Abstract*—In a phase controlled rectifier, the fastest response can be achieved by predictive current control without any overshoot. However, any error in the load parameters can cause steady state errors between a reference current and the feedback current because this current control scheme depends on the mathematical relationships between the output current, the firing angle, and the power source voltage. Thus, in the predictive current control, an accurate parameter is necessary for attaining a zero steady-state error. In this paper, the load resistance and inductance are estimated using the least square method of an online parameter calculation based on digitally sampled instantaneous voltage and currents. For the careful sampling of data and the reduction of the calculation time, a new timer-based gating algorithm is proposed and explained in detail. Using the proposed algorithm, the fastest current control performance in the transient state is obtained by the online correction of load parameters in various simulations and experimental results.**

***Index Terms*—Parameter estimation, phase controlled rectifier, predictive current control.**

I. Introduction

NUMEROUS thyristor converters are still in use in many process control lines as main motor drives for the variable speed operation of existing dc motors. For example, a rolling mill driven by a dc motor requires a very fast torque control response to cope with the impact load at the moment of strip (material) entrance. Other important applications such as high power magnetic power supplies and high voltage dc (HVDC) transmission systems also require accurate and fast control of load currents. [1], [2].

In a phase controlled rectifier, conventional armature current control is usually accomplished with a proportional–integral (PI) controller adjusted for the desired response in the continuous current mode. [3] However, the nonlinear characteristic due to the discontinuity in the armature current deteriorates the current control response [3], [4]. An innovative predictive current control algorithm was proposed in [4] by calculating the predictive current in real time and comparing with the actual current. The fastest current control response can be achieved by predictive current control without any overshoot [4]–[7]. However, accurate parameters are necessary for a predictive current controller because any inaccuracy in the load parameters can cause steady state errors between the reference and the feedback current [8], [9]. Although an adaptive parameter estimation is proposed for time optimal control in [10], only the load resistance is estimated using computer simulation.

As the conventional predictive current controller compares a predicted (calculated) current with the actual (sampled) current, a short sampling period is required for accurate pulse firing [4]–[6]. Furthermore, it is difficult to ensure additional time for correcting the load parameter. Another predictive current control scheme uses a hardware timer for pulse firing based on the calculation of the optimal firing angle. However, this scheme uses an error compensator to avoid the difference between a reference current and feedback current. As a result, a current control error is inevitable during a transient state such as a current reference change [7].

In this paper, the load parameters are estimated online using the least square method based on the instantaneous sampling of the voltage and current. Further, a gating algorithm for the firing angle calculation is proposed for the fastest current control performance in every possible transient condition. The performance of the proposed algorithm is verified through various simulations and experiments.

II. Predictive Current Control

Fig. 1 shows a three phase controlled dual thyristor converter with a dc load. In (1), the average output voltage is a function of the firing angle α when the converter currents are in the continuous conduction mode. However, in (2), it is a function of the firing angle α and extinction angle β in the discontinuous conduction mode

$$\overline{v_{\rm dc}} = \frac{3\sqrt{2}V}{\pi}\cos\alpha \tag{1}$$

$$\overline{v_{\rm dc}} = \frac{3\sqrt{2}V}{\pi}\int_{\alpha-\pi/6}^{\beta-\pi/6}\cos\omega t d(\omega t) \tag{2}$$

where α : firing angle

β : extinction angle.

In Fig. 1, it is assumed that the thyristors in the system act as ideal switches. When current flows into the load, an equivalent

Manuscript received July 15, 2005; revised May 31, 2006. This work was supported by a grant from Kwangwoon University. Recommended for publication by Associate Editor B. Fahimi.

S.-J. Jeong is with Hyundai Heavy Industries Co., Ulsan 682-792, Korea (e-mail: good2sejong@hotmail.com).

S.-H. Song is with the Department of Electrical Engineering, Kwangwoon University, Seoul 139-701, Korea (e-mail: ssh@kw.ac.kr).

Color versions of one or more of the figures in this paper are available online at http://ieeexplore.ieee.org.

Digital Object Identifier 10.1109/TPEL.2007.904235

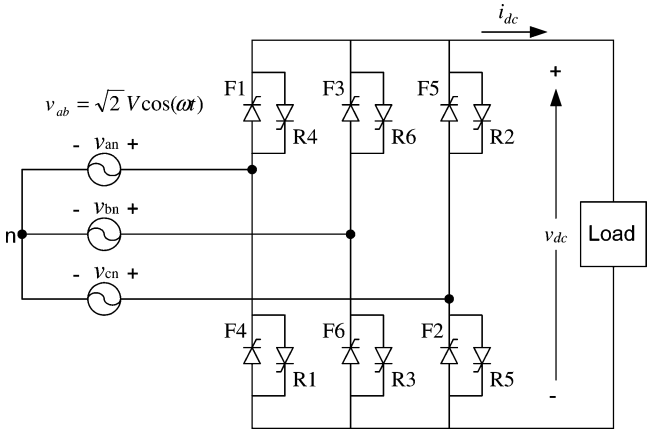

Fig. 1. Circuit of a dual thyristor converter with a dc load.

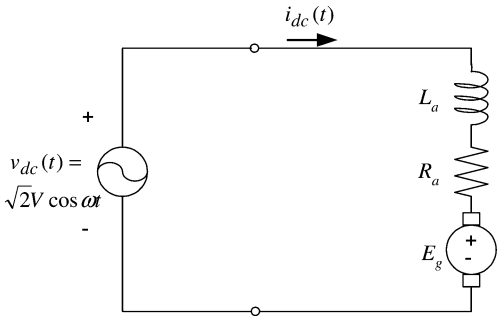

Fig. 2. Equivalent circuit of a dc drive during the turn-on period of a set of thyristors.

circuit can be described as shown in Fig. 2, and the relationship between the voltage and current is expressed as

$$v_{\rm dc}(t) = R_a i_{\rm dc}(t) + L_a \frac{di_{\rm dc}(t)}{dt} + E_g. \tag{3}$$

Generally, it is assumed that the mechanical time constant associated with a motor is usually much larger than the control period. Hence, the speed or back emf is not expected to change. The output current—the solution of (3)—is represented by three terms as shown in (4) [4]

$$i_{\rm dc}(t) = I_1\cos(\omega t - \phi) + I_2 e^{-\frac{R_a}{L_a}t} + I_3 \tag{4}$$

where $I_1 = \frac{\sqrt{2}V}{Z}$ and the equation shown at the bottom of the page.

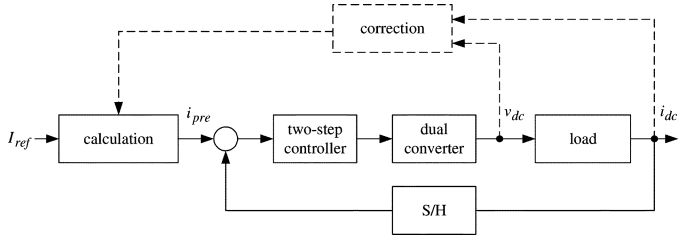

Fig. 3. Block diagram of a predictive controller.

Fig. 3 shows the block diagram of a conventional predictive current controller. The predictive current controller predicts the current shape of the next firing mode from a reference current, power source, load parameters, and back-emf. A two-step (on/off) controller compares the sampled converter current $i_{\rm dc}$ with the precalculated current $i_{\rm pre}$ and generates the gating signal of a converter just after $i_{\rm dc}$ intersects with $i_{\rm pre}$. If all the parameters are exactly known and the sampling (comparison) time is short enough, predictive current control can be used to achieve the fastest current response in a phase controlled rectifier [4].

For accurate firing with conventional predictive current control, a short sampling period is required for the calculation of $i_{\rm pre}$ and its comparison with $i_{\rm dc}$. However, the actual implementation of this predictive current control required a sampling time of 55.55 [μs] (electrical degree of 1.2°) even though a 32–b DSP (digital signal processor) was used [5]. As a result, the resolution of the change in the gating angle was limited to the sampling time and it was difficult to find additional time to develop a better algorithm such as one for parameter correction. If the load parameters are unknown or different from the actual values, which is typical during the commissioning, a steady state current error is inevitable. Although the need of parameter correction block (dotted line in Fig. 3) was introduced in [4], the implementation method of correction and any results about the parameter correction could not found.

III. Proposed Predictive Current Controller With Online Parameter Estimator

Fig. 4 shows the proposed current control block diagram with timer gating and online parameter correction. The calculation time for parameter correction is assured by a modification of the gating algorithm—the pre-calculation of the firing angle instead of the sampling-based comparison method. The load parameters can be calculated by the least square method from the

$$I_2 = \begin{cases} \frac{\rho\pi}{3}\left[I_{\rm ref} - I_3 - \frac{3}{\pi}I_1\cos(\alpha-\phi)\right] e^{\rho\alpha} / \left(e^{\frac{\pi}{6}\rho} - e^{-\frac{\pi}{6}\rho}\right) & : \text{continuous conduction mode} \\ \left[-I_3 - I_1\cos\left(\alpha - \frac{\pi}{6} - \phi\right)\right] e^{\rho\alpha} & : \text{discontinuous conduction mode} \end{cases}$$

$$I_3 = -\frac{E_g}{R}$$

$$Z = \sqrt{R_a^2 + (\omega L_a)^2}, \quad \rho = \frac{R_a}{\omega L_a}, \quad \phi = \tan^{-1}\left(\frac{1}{\rho}\right), \alpha: \text{ firing angle}$$

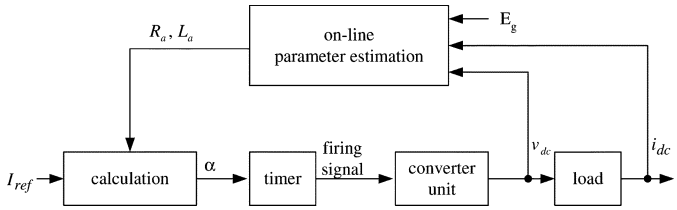

Fig. 4. Proposed predictive current controller with an online parameter estimator.

digitally sampled signals, namely, the load voltage, load current, and back-emf. The voltage equation can be approximated as shown in (5) with a sampling period T_s

$$v_{\rm dc}[n] = R_a i_{\rm dc}[n] + L_a \frac{i_{\rm dc}[n+1] - i_{\rm dc}[n-1]}{2T_s} + E_g. \quad (5)$$

From (5), the load parameters are calculated from a voltage and current matrix

$$\begin{bmatrix} R_a \\ L_a \end{bmatrix} = \left[\mathbf{I}^T\mathbf{I}\right]^{-1}\mathbf{I}^T\mathbf{V} \quad (6)$$

where you have the equation shown at the bottom of the page.

In this method, sampling points are carefully selected because the approximation error of a differential term becomes large due to a sudden change in the current slope near the firing point.

Prior to the accurate calculation of the firing angle, many conditions should be considered. When the reference current varies in the continuous conduction mode, the calculation method of the intermediate firing angle α_x is shown [7]. However, it should be considered that the reference current varies from the discontinuous conduction mode to the continuous conduction mode and vice-versa. Fig. 5 shows the relation between the intersection point and the intermediate firing angle. When the intersection point is above zero, the intersection point of two currents has an accurate firing point [as shown in Fig. 5(a)]. However, if the intersection point is below zero, the firing angle is recalculated with a zero initial current [as shown in Fig. 5(b)].

Fig. 6 shows the flow chart for the calculation of the firing angle for both the steady state and transient state. In each current control period, the firing angle is calculated in the steady state. If the reference current remains unchanged, α_2 becomes the firing angle. In a situation involving a changed reference current for the continuous or discontinuous conduction mode, the intersection point I_i is calculated by considering that the predicted current would intersect with the load current. Thus, if I_i is above zero, α_i becomes the firing angle. However, if I_i is below zero, we can obtain the intermediate firing angle α_x using a zero initial current.

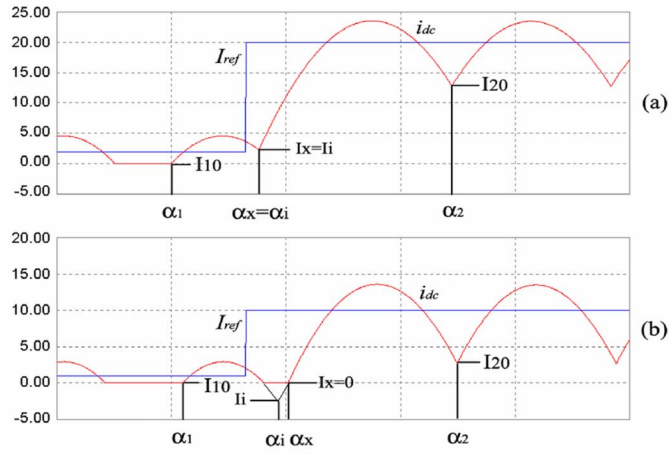

Fig. 5. Transition of the firing angle (a) with the intersection point above zero and (b) with the intersection point below zero.

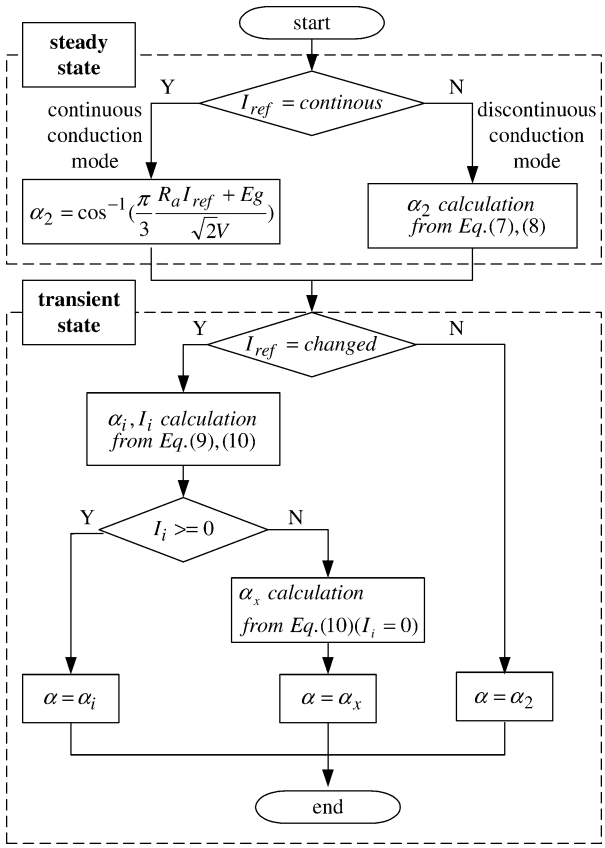

Fig. 6. Flow chart of firing angle calculation.

$$\mathbf{V} = [v_{\rm dc}[2] - E_g, v_{\rm dc}[3] - E_g, \ldots v_{\rm dc}[N-1] - E_g]^T$$

$$\mathbf{I} = \begin{bmatrix} i_{\rm dc}[2] & i_{\rm dc}[3] & \cdots & i_{\rm dc}[N-1] \\ i_{\rm dc}[3] - i_{\rm dc}[1] & i_{\rm dc}[4] - i_{\rm dc}[2] & \cdots & i_{\rm dc}[N] - i_{\rm dc}[N-2] \end{bmatrix}^T$$

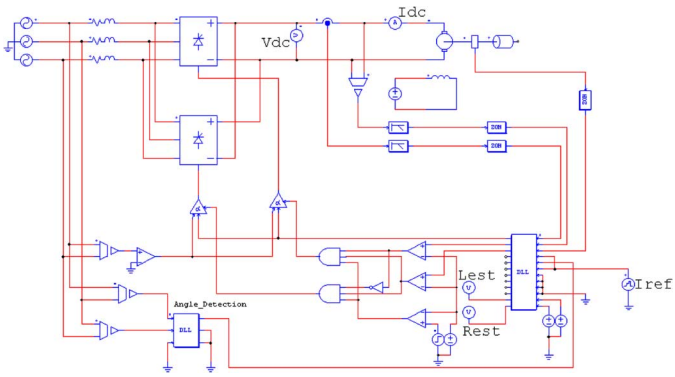

Fig. 7. Simulation circuit using a dc-motor load.

When the reference current is in the discontinuous conduction mode, the firing angle is obtained by solving (7) and (8) iteratively. The values of α and β are then substituted in (4)

$$I_1 \cos\left(\alpha - \frac{\pi}{6} - \phi\right) - \left[I_3 + I_1 \cos\left(\beta - \frac{\pi}{6} - \phi\right)\right] e^{\rho(\beta-\alpha)} + I_3 = 0. \quad (7)$$

From the average output voltage condition

$$\frac{\pi}{3}(R_a I_{\text{ref}} + E_g) = \sqrt{2}V\left[\sin\left(\beta - \frac{\pi}{6}\right) - \sin\left(\alpha - \frac{\pi}{6}\right)\right] + E_g\left(\alpha - \beta + \frac{\pi}{3}\right). \quad (8)$$

When the reference current changes, the optimum firing angle in the transient state differs from the firing angle in the steady state; this is because a change in the average current of an inductor requires additional voltage $(L_a(d\overline{i_{\text{dc}}})/(dt))$.

In Fig. 5, the intersecting angle α_i and current I_i are obtained by solving the two equations derived by substituting the current reference, steady state firing angle α_2, and intersecting angle α_i in (4)

$$I_i = I_1 \cos\left(\alpha_i + \frac{\pi}{6} - \phi\right) + I_2 e^{-\rho(\alpha_i + \frac{\pi}{6})} + I_3 \quad (9)$$

$$I_{20} = I_1 \cos\left(\alpha_2 - \frac{\pi}{6} - \phi\right) + I_{2\text{new}} e^{-\rho\left(\alpha_2 - \frac{\pi}{6}\right)} + I_3 \quad (10)$$

where

$$I_{2\text{new}} = \left[I_i - I_1 \cos\left(\alpha_i - \frac{\pi}{6} - \phi\right) - I_3\right] e^{\rho(\alpha_i - \frac{\pi}{6})}.$$

If I_i is below zero, the firing angle must be recalculated from (10) with a zero initial current $(I_i = 0)$.

IV. Simulation Results

A simulation block diagram is shown in Fig. 7. Further, the motor parameters used in this simulation are shown in Table I. The commercial simulation tool PSIM is used with a DLL (a C-language based dynamic link library) function.

TABLE I
Motor Parameters

Rating Power	5.5 [kW]
Rating Voltage	220 [V]
Rating Current	32 [A]
Resistance R_a	1.0 [Ω]
Inductance L_a	10 [mH]

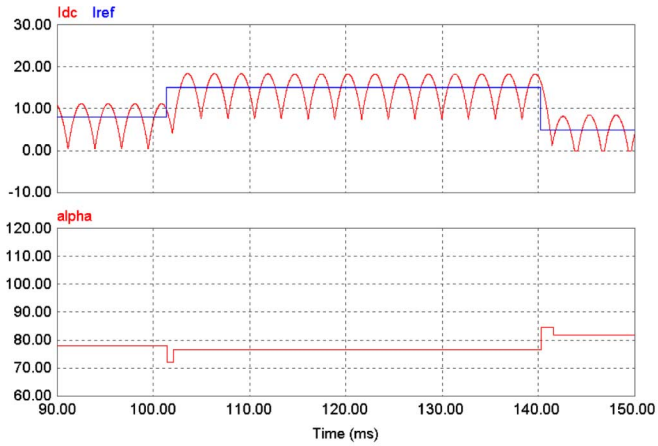

Fig. 8. Current control response and firing angle with 100% parameters.

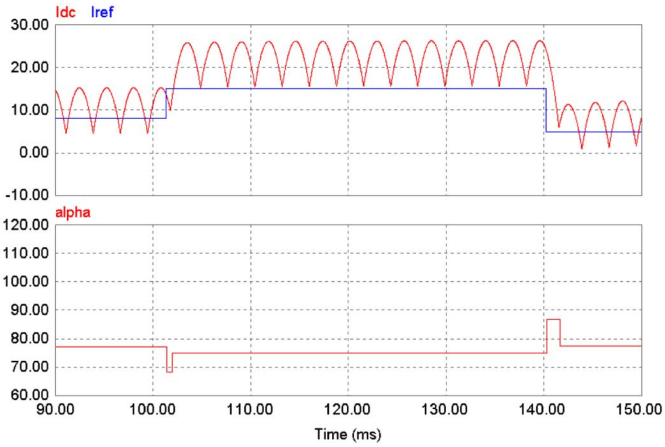

Fig. 9. Current control response and firing angle with 150% parameters.

Fig. 8 shows the ideal current control response when the predictive current controller is implemented with 100% parameters. However, the current control response shows a steady state error between the reference current and the feedback current when the predictive current controller is implemented with 150% parameters (as shown in Fig. 9).

Fig. 10 shows the current control response when a PI controller compensates the predictive current controller. It shows a zero steady state error but an overshoot appears with a variation in the reference current.

Fig. 11 shows the performance of the proposed predictive current controller with the online parameter estimator. After the estimated parameter converged, there was no indication of an

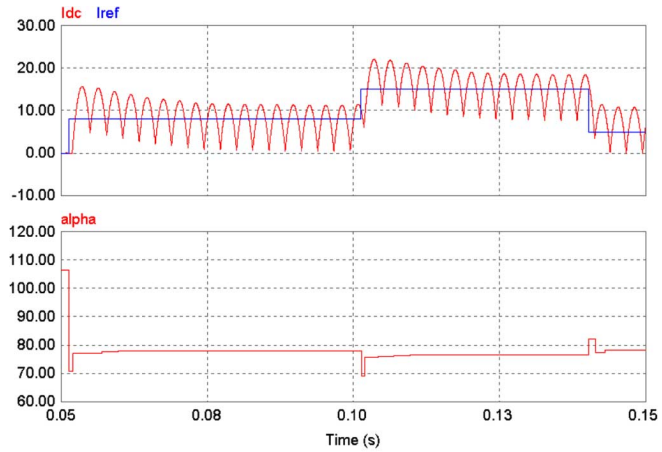

Fig. 10. Current control response and firing angle with a PI controller.

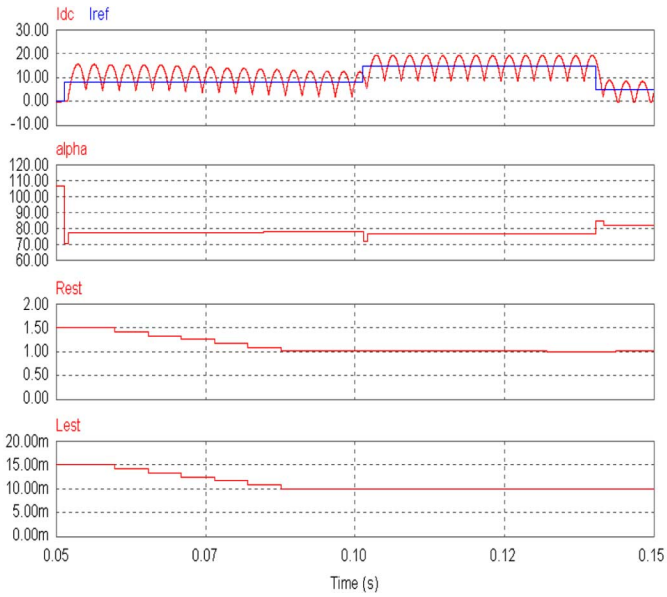

Fig. 11. Current control response, firing angle, and estimated R and L with the online parameter estimator.

overshoot and the steady state error that initially appeared before estimation started.

V. Experimental Results

The experimental setup is shown in Fig. 12. The main control board is based on a 32 b floating point DSP, the TMS 320C31 CPU, which has two timers with a time increment step of 80 ns [11]. An advanced PLL algorithm based on the rotating reference frame is utilized [12]. The sampling frequency for the parameter estimation is 10.8 [kHz] and the calculated parameter is updated every 5.5 [ms].

The proposed calculation algorithm for the firing angle is verified under various conditions: the reference current varies from discontinuous to continuous (0 [A] $\rightarrow$ 8 [A]), in the continuous mode (8 [A] $\rightarrow$ 15 [A]), and from continuous to discontinuous in the conduction mode (15 [A] $\rightarrow$ 5 [A]).

Fig. 12. Experimental setup.

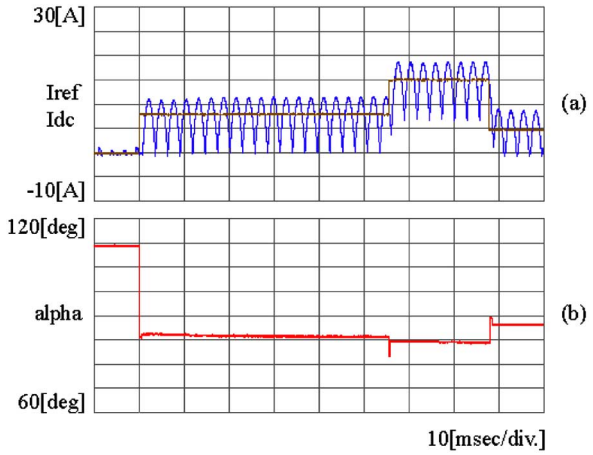

Fig. 13. (a) Current control response and (b) firing angle with 100% parameters.

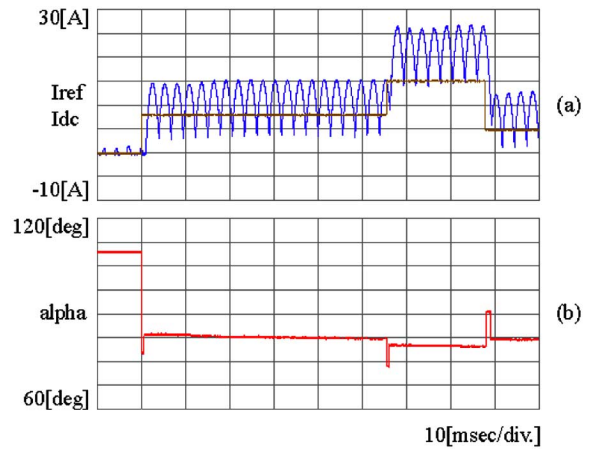

Fig. 14. (a) Current control response and (b) firing angle with 150% parameters.

Figs. 13 and 14 show the current control response and the firing angle with fixed parameters of 100% and 150%, respectively. In Fig. 13(a), the overshoot and steady state error are not visible in the current control response with 100% parameters. However, the current control response with 150% parameters

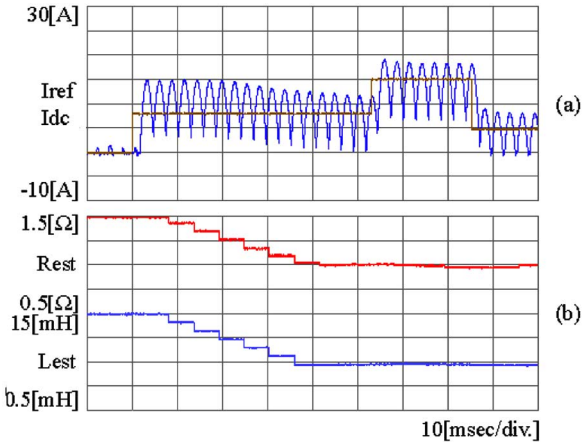

Fig. 15. (a) Current response by the controller parameter and (b) estimated R, L.

has a steady state error, as shown in Fig. 14(a). In Fig. 13(b), a step change in the firing angle appears as a result of the step change in the reference current.

Fig. 15 shows the performance of the proposed predictive current controller with the online parameter estimator. A steady state error appears in the current control response for the incorrect initial parameters of 150% R and L values. After the convergence of the estimated parameter, there is no indication of the overshoot and the steady state error that initially appeared before the start of estimation. The load parameters converged to the actual value in approximately 35 [ms].

VI. Conclusion

The steady state error of the predictive current control performance is eliminated by an online parameter estimator of the dc load in a phase controlled rectifier. The combination of a fast predictive current control response and the zero steady state error using parameter estimation demonstrated an ideal current control response in the simulation and the experiment. A software-based phase locked loop is utilized for the implementation of real-time control, and the firing angle for timer gating is analytically calculated from the state equations not only for steady state but also for the transient state. The result of this study can be applied to the R–L–Emf loads that require a high performance current (torque) control response.

References

[1] S. Song, "Current control of 12-pulse regenerative converter for high current magnetic power supply," *Elect. Power Comp. Syst.*, vol. 34, no. 8, pp. 917–926, 2006.

[2] B.-M. Yang, C.-K. Kim, G.-J. Jung, and Y.-H. Moon, "Verification of hybrid real time HVDC simulator in Cheju-Haenam HVDC system," *J. Elect. Eng. Technol.*, vol. 1, no. 1, pp. 23–27, 2006.

[3] T. Ohmae, T. Matsuda, T. Suzuki, N. Asawa, K. Kamiyama, and T. Konishi, "Microprocessor-controlled fast response speed regulator with dual mode current loop for DCM drives," *IEEE Trans. Ind. Appl.*, vol. IA-16, no. 3, pp. 388–394, May/Jun. 1980.

[4] R. Kennel and D. Schroeder, "Predictive control strategy for converters," *IFAC Contr. Power Electron. Elect. Drives*, pp. 415–422, 1983.

[5] J.-K. Ji, S.-H. Song, S.-K. Sul, and M.-H. Park, "DSP-based self-tuning IP speed controller for rolling mill DC drive," in *Proc. Power Conv. Conf.*, Yokohama, Japan, 1993, pp. 303–308.

[6] J.-K. Ji and S.-K. Sul, "Operation analysis and new current control of parallel connected dual converter system without interphase reactors," in *Proc. IECON'99*, 1999, vol. 1, pp. 235–240.

[7] T. D. Collings and W. J. Wilson, "A fast-response current controller for microprocessor-based SCR-dc motor drives," *IEEE Trans. Ind. Appl.*, vol. 27, no. 5, pp. 921–927, Sep./Oct. 1991.

[8] D. Drake and P. Lindon, "Improvement of current loop response of thyristor DC drive by time-domain approximation," *Proc. IEEE*, vol. 135, no. 5, pp. 261–268, May 1988.

[9] Z. Kovacic, S. Bogdan, Z. Ban, and P. Cmosija, "Adaptive time optimal control of thyristor converter current," in *Proc. EPE Conf.*, 1993, pp. 41–46.

[10] W. F. Ray and A. Moussi, "Optimal-current Control of converter-fed DC motors, Part 2: General Case," *Proc. Inst. Elect. Eng.*, vol. 141, no. 5, pp. 249–258, 1994.

[11] S.-J. Jeong and S.-H. Song, "Improvement of predictive current control performance using on-line parameter estimation in phase controlled rectifier," in *Proc. KIPE 2002 Power Electron. Autumn Conf.*, 2002, pp. 140–143.

[12] S.-J. Lee, J.-K. Kang, and S.-K. Sul, "A new phase detecting method for power conversion systems considering distorted conditions in power system," in *Proc. IEEE IAS Annu. Meeting*, 1999, vol. 4, pp. 2167–2172.

Se-Jong Jeong (S'03) was born in Jeonju, Korea, in 1975. He received the B.S. and M.S. degrees in electrical engineering from Chonbuk National University, Jeonju, Korea, in 2001 and 2003, respectively.

He is currently a Researcher with Hyundai Heavy Industries Co., Ltd., Ulsan, Korea. His research interest is power electronics, especially in the area of adjustable-speed ac drives and high-performance electrical machine drives.

Seung-Ho Song (S'92–M'95) received the B.S., M.S., and Ph.D. degrees in electrical engineering from Seoul National University, Seoul, Korea, in 1991, 1993, and 1999, respectively.

In 1992, he joined POSCON as a Research Engineer, where he worked on the development of dc and ac machine drives for steel rolling mill applications until 1995. From 2000 to 2006, he was an Assistant Professor in the Division of Electronics and Information, Chonbuk National University, Jeonju, Korea. Also he was a Visiting Professor in WEMPEC, University of Wisconsin, Madison, from 2004 to 2005. Currently, he is an Associate Professor in the Department of Electrical Engineering, Kwangwoon University, Seoul. His research interests include electric machine drives and renewable energy conversion.